

## University of Wollongong - Research Online

### Thesis Collection

Title: The impact of detector volume on penumbral dose prediction in a 6 MV radiation therapy X-ray beam

Author: Johnson Yuen

Year: 2009

Repository DOI:

#### Copyright Warning

You may print or download ONE copy of this document for the purpose of your own research or study. The University does not authorise you to copy, communicate or otherwise make available electronically to any other person any copyright material contained on this site.

You are reminded of the following: This work is copyright. Apart from any use permitted under the Copyright Act 1968, no part of this work may be reproduced by any process, nor may any other exclusive right be exercised, without the permission of the author. Copyright owners are entitled to take legal action against persons who infringe their copyright. A reproduction of material that is protected by copyright may be a copyright infringement. A court may impose penalties and award damages in relation to offences and infringements relating to copyright material.

Higher penalties may apply, and higher damages may be awarded, for offences and infringements involving the conversion of material into digital or electronic form.

**Unless otherwise indicated, the views expressed in this thesis are those of the author and do not necessarily represent the views of the University of Wollongong.**

Research Online is the open access repository for the University of Wollongong. For further information contact the UOW Library: [research-pubs@uow.edu.au](mailto:research-pubs@uow.edu.au)

2009

## The impact of detector volume on penumbral dose prediction in a 6 MV radiation therapy X-ray beam

Johnson Yuen  
*University of Wollongong*

Follow this and additional works at: <https://ro.uow.edu.au/theses>

### University of Wollongong

#### Copyright Warning

You may print or download ONE copy of this document for the purpose of your own research or study. The University does not authorise you to copy, communicate or otherwise make available electronically to any other person any copyright material contained on this site.

You are reminded of the following: This work is copyright. Apart from any use permitted under the Copyright Act 1968, no part of this work may be reproduced by any process, nor may any other exclusive right be exercised, without the permission of the author. Copyright owners are entitled to take legal action against persons who infringe their copyright. A reproduction of material that is protected by copyright may be a copyright infringement. A court may impose penalties and award damages in relation to offences and infringements relating to copyright material.

Higher penalties may apply, and higher damages may be awarded, for offences and infringements involving the conversion of material into digital or electronic form.

Unless otherwise indicated, the views expressed in this thesis are those of the author and do not necessarily represent the views of the University of Wollongong.

### Recommended Citation

Yuen, Johnson, The impact of detector volume on penumbral dose prediction in a 6 MV radiation therapy X-ray beam, MSc thesis, School of Engineering Physics, University of Wollongong, 2009.  
<http://ro.uow.edu.au/theses/851>

## **NOTE**

This online version of the thesis may have different page formatting and pagination from the paper copy held in the University of Wollongong Library.

## **UNIVERSITY OF WOLLONGONG**

### **COPYRIGHT WARNING**

You may print or download ONE copy of this document for the purpose of your own research or study. The University does not authorise you to copy, communicate or otherwise make available electronically to any other person any copyright material contained on this site. You are reminded of the following:

Copyright owners are entitled to take legal action against persons who infringe their copyright. A reproduction of material that is protected by copyright may be a copyright infringement. A court may impose penalties and award damages in relation to offences and infringements relating to copyright material. Higher penalties may apply, and higher damages may be awarded, for offences and infringements involving the conversion of material into digital or electronic form.

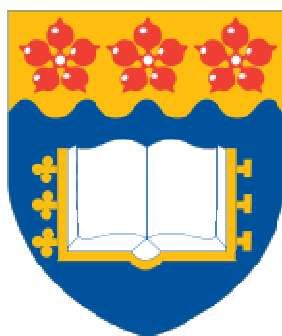
**The impact of detector volume on penumbral dose prediction  
in a 6 MV radiation therapy X-ray beam**

A thesis submitted in partial fulfilment of the requirements for the award of the degree

MASTER OF SCIENCE - RESEARCH

From

THE UNIVERSITY OF WOLLONGONG



By

Johnson Yuen, BSc (Hon Class 1)

School of Engineering Physics

2009

## **Thesis Certification**

### **CERTIFICATION**

I, Johnson Yuen, declare that this thesis, submitted in fulfilment of the requirements for the award of Masters of Research in Medical Physics, in the Department of Engineering, University of Wollongong, is wholly my own work unless otherwise referenced or acknowledged. The document has not been submitted for qualifications at any other academic institution

---

Signed

Johnson Yuen

3<sup>rd</sup> March 2009

## TABLE OF CONTENTS

<b>CHAPTER 1: INTRODUCTION .....</b>	<b>1</b>
1.0 INTRODUCTION TO THE THESIS .....	1
1.1 WHY IS RADIOTHERAPY IMPORTANT? .....	2
1.2 HOW IS MEDICAL RADIATION DELIVERED IN RADIOTHERAPY? .....	6
1.3 MODERN ADVANCES IN LINAC RADIOTHERAPY .....	14
<b>CHAPTER 2: LITERATURE REVIEW .....</b>	<b>20</b>
2.1 INTRODUCTION TO SCOPE OF STUDY .....	20
2.2 PHYSICS IN THE PENUMBRAL REGION .....	24
2.3 REVIEW OF DETECTORS .....	29
2.4 REVIEW OF THE DIAMOND DETECTOR .....	37
2.5 REVIEW OF THE MULTILEAF COLLIMATOR (MLC) .....	44
<b>CHAPTER 3: EXPERIMENTAL METHOD .....</b>	<b>54</b>
3.1 EQUIPMENT USED FOR DATA COLLECTION .....	54
3.2 METHOD OF DATA COLLECTION .....	64
3.3 DATA ANALYSIS AND PROCESSING .....	74
3.4 RADIOTHERAPY TREATMENT PLANNING SYSTEM MODELLING .....	76
3.5 RADIOTHERAPY TREATMENT PLANNING SYSTEM PLANNING .....	83
3.6 DISCUSSION OF BEAM PARAMETERS USED .....	87
<b>CHAPTER 4: ANALYSIS OF THE CURVE PROPERTIES OF THE DOSE PROFILES MEASURED WITH DIFFERENT DETECTORS .....</b>	<b>91</b>
4.1 OVERVIEW .....	91
4.2 SENSITIVE DETECTOR DIAMETER DATA .....	92
4.3 INFLECTION POINT OF PROFILES .....	94
4.4 INTERSECTION POINT OF DETECTORS .....	101
4.4 DISCUSSION OF INTERSECTION AND INFLECTION POINTS .....	106
4.5 CONCLUSIONS OF INTERSECTION AND INFLECTION POINTS .....	107
<b>CHAPTER 5: DERIVING VIRTUAL ZERO DETECTOR VOLUME PROFILES BASED ON EXTRAPOLATION OF DATA FROM MULTIPLE DETECTOR DIAMETERS .....</b>	<b>110</b>
5.1 THEORY .....	110
5.2 METHOD .....	111
5.3 RESULTS .....	112
5.4 VALIDATION OF METHOD .....	116
5.5 DISCUSSION .....	124
5.6 CONCLUSIONS .....	129
<b>CHAPTER 6: DERIVING VIRTUAL ZERO DETECTOR VOLUME PROFILES BY DECONVOLUTION BASED ON DETECTOR DATA .....</b>	<b>131</b>

6.1	THEORY .....	131
6.2	METHOD .....	134
6.3	RESULTS .....	139
6.4	DISCUSSION .....	144
6.5	CONCLUSIONS .....	147
<b>CHAPTER 7: ANALYSIS OF THE EFFECT OF DETECTOR VOLUME ON SMEARING OF DOSE PROFILES .....</b>		<b>150</b>
7.1	PENUMBRA ANALYSIS .....	150
7.2	FIELD SIZE ANALYSIS.....	153
7.3	DOSE ANALYSIS .....	156
7.4	DISCUSSION OF PROFILE PARAMETERS.....	164
7.5	CONCLUSION .....	167
<b>CHAPTER 8: A NON-LINEAR EXTRAPOLATION EQUATION USING PENUMBRA DATA TO CALCULATE VIRTUAL ZERO DETECTOR VOLUME PENUMBRAS.....</b>		<b>174</b>
8.1	THEORY .....	174
8.2	METHOD .....	177
8.3	RESULTS .....	182
8.4	DISCUSSION .....	188
8.4	CONCLUSIONS .....	191
<b>CHAPTER 9: THE PINNACLE SOURCE SIZE MODEL WITH RESPECT TO THE DETECTOR EFFECT .....</b>		<b>194</b>
9.1	INTRODUCTION .....	194
9.2	METHOD .....	195
9.3	RESULTS.....	196
9.4	DISCUSSION .....	206
9.5	CONCLUSIONS .....	208
<b>CHAPTER 10: EFFECT OF DETECTOR VOLUME ON ISODOSE DISTRIBUTIONS .....</b>		<b>214</b>
10.1	OVERVIEW .....	214
10.2	METHOD .....	214
10.3	RESULTS: PLAN 4FS1 .....	217
	RESULTS: 4 FIELD 10×10 CM2 PLAN.....	226
	RESULTS: 4 FIELD PROSTATE PLAN .....	231
	DISCUSSION .....	235
	CONCLUSION .....	237
<b>CHAPTER 11: CONCLUSION AND FUTURE WORK.....</b>		<b>241</b>
11.1	CONCLUSIONS .....	241
11.2	POTENTIAL CLINICAL SIGNIFICANCE .....	244
11.3	FUTURE WORK .....	246

<b>APPENDIX A: THE EFFECT OF JAW POSITION FOR MLC FIELDS IN THE CENTRAL AXIS .....</b>	<b>252</b>
<b>APPENDIX B: PROFILE MEASUREMENTS ALONG LEAF-END JUNCTION.....</b>	<b>256</b>
<b>APPENDIX C: INVESTIGATION INTO THE EFFECT OF END-LEAF OFFSET .....</b>	<b>260</b>
<b>APPENDIX D: EFFECT OF LATERAL ELECTRON EQUILIBRIUM AND BEAM QUALITY ESTIMATES WITH FIELD SIZE .....</b>	<b>268</b>
<b>APPENDIX E: BASIC MATHEMATICAL MODELLING OF THE CENTRAL AXIS DOSE VERSUS THE OUT OF FIELD DOSE .....</b>	<b>273</b>
<b>APPENDIX F: MCC FILE FORMAT.....</b>	<b>279</b>
<b>APPENDIX G: BEAM QUALITY ACROSS THE PROFILE .....</b>	<b>284</b>
<b>APPENDIX H: RESULTS OF SOURCE SIZE SURVEY .....</b>	<b>289</b>
<b>APPENDIX I: CODE FOR DECONVOLUTION .....</b>	<b>295</b>
<b>APPENDIX J: CODE FOR PLANAR DOSE.....</b>	<b>298</b>
<b>REFERENCES.....</b>	<b>300</b>



## LIST OF FIGURES

FIGURE 1.1: CAUSES OF DEATH FOR MALES, 2005 DATA FROM (AIHW 2005). THE LEADING CAUSE OF DEATH FOR FEMALES FOLLOWS A SIMILAR CURVE, AND DATA FOR THIS CAN BE FOUND IN THE LITERATURE. ....	3
FIGURE 1.2: COMPARISON OF DATA FROM DEPTH DOSE CURVES OF 100 kV PHOTONS (KOCH & STERZEL THERAPIX C100) AND 6MV PHOTONS (CLINAC 600C) AT ST. GEORGE HOSPITAL .....	8
FIGURE 1.3: FIGURE OF A TYPICAL LINEAR ACCELERATOR, ADAPTED FROM (VAN-DYK 1999) .....	9
FIGURE 1.4: ILLUSTRATION OF THE DIFFERENCE BETWEEN CONVENTIONAL AND CONFORMAL THERAPY (WEBB 1993) .....	14
FIGURE 1.5: DIAGRAM SHOWING FIVE INTENSITY MODULATED PROFILES TO TREAT THE TARGET VOLUME (HATCHED), ILLUSTRATION FROM (BRAHME 1988) .....	15
FIGURE 1.6: AN ISODOSE CURVE FROM A HEAD AND NECK PLAN WITH IMRT THAT ILLUSTRATES THE SPARING OF THE PAROTID GLANDS, ILLUSTRATION FROM (IMRT-CWG 2001) .....	16
FIGURE 1.7: DOSE-RESPONSE CURVE FOR TUMOUR CONTROL AND NORMAL TISSUE RESPONSE. SMALL ARROW INDICATES THE EFFECT ON DOSE RESPONSE WITH 5% CHANGE IN DOSE. ILLUSTRATION FROM (VAN-DYK 1999) .....	17
FIGURE 1.8: FIGURE SHOWING THE TUMOUR CELL AND ILLUSTRATING THE GTV (A), CTV (B), AND THE PTV (C). DIAGRAM FROM (VAN-DYK 1999). ....	18
FIGURE 2.1: SCHEMATIC DIAGRAM OF THE COLLIMATOR GEOMETRY ILLUSTRATING THE VARIABLES FOR THE CALCULATION OF GEOMETRIC PENUMBRA, FROM (AAPM 2008). NOTE THAT THE SCD FOR VARIAN MACHINES IS 38.0 CM FOR THE X JAW AND 48.3 CM FOR THE Y JAW .....	26
FIGURE 2.2: FOR (A), THE FIELD SIZE CORRESPONDS TO CHARGED PARTICLE EQUILIBRIUM AND FWHM CORRESPONDS TO 50% DOSE LEVEL OF CPE. FOR (B), THE FIELD SIZE IS OF THE SAME ORDER AS CPE AND THE PENUMBRA FROM THE OPPOSING FIELD OVERLAPS TO CAUSE A SMALL ERROR. FOR (C), FWHM IS OVERESTIMATED WITH RESPECT TO 50% DOSE LEVELS OF CPE SINCE THE RESULTING CURVE HAS A LOWER MAXIMUM VALUE. ADAPTED FROM (DAS, DING ET AL. 2007) .....	28
FIGURE 2.3: THE 80-20% PENUMBRA PLOTTED AGAINST THE DETECTOR SIZE A FOR A 6 MV BEAM. IT WAS FOUND (PAPPAS, MARIS ET AL. 2006) THAT THE USE OF A DETECTOR LESS THAN 0.5 MM WOULD MINIMISE THE VOLUME EFFECT FROM A DETECTOR. ....	31
FIGURE 2.4: MEASURED RESPONSE OF THE DIAMOND DETECTOR AT PHOTON ENERGIES FROM 4-25 MV WITH THE STOPPING POWER RATIO OF WATER/CARBON AND OF WATER/AIR FROM (LAUB, KAULICH ET AL. 1997) .....	40
FIGURE 2.5: LOGIC DIAGRAM HIGHLIGHTING THE RELATIONSHIP OF RECOMBINATION TIME, CONDUCTIVITY, DOSE RATE, AND THE NUMBER OF HOLES IN THE DIAMOND DETECTOR .....	42
FIGURE 2.6: ILLUSTRATION OF A GENERAL LEAF FROM A MLC WITH A CURVED END, ADAPTED FROM (AAPM_TG_50 2001) .....	46
FIGURE 2.7: CROSS-SECTIONAL VIEWS OF THE VARIAN 120-LEAF MLC WITH THE (A) END VIEW AND THE (B) SIDE VIEW (KIM, SIEBERS ET AL. 2001) .....	48
FIGURE 2.8: FOR ROUNDED LEAF END MLCs, THE ACTUAL FIELD SIZE CALIBRATION DIFFERS FOR LIGHT ( $X_{\text{LIGHT}}$ ) AND RADIATION FIELD ( $X_{\text{RAD}}$ ) EDGES, AND DEPENDS IN A COMPLEX WAY ON THE MOTION OF THE LEAVES ( $X_{\text{MLC}}$ ) (GRAVES, THOMPSON ET AL. 2001) .....	50

FIGURE 2.9: RADIATION FIELD MEASUREMENTS OF ORIGINAL AND CORRECTED AVERAGES (RIGHT)	
BETWEEN MEASURED AND READOUT (GRAVES, THOMPSON ET AL. 2001) .....	52
FIGURE 3.1: MLC SHAPER OPTIONS.....	55
FIGURE 3.2: PTW WATER TANK.....	56
FIGURE 3.3: MP3 ELECTROMETER (ABOVE) AND MP3 CONTROL UNIT (BELOW) .....	56
FIGURE 3.4: COMPARISON BETWEEN PDD DATA FOR DIAMOND DETECTOR AND 0.125 CC IONISATION	
CHAMBER FOR JAW DEFINED 10x10 CM <sup>2</sup> FIELD .....	61
FIGURE 3.5: DERIVATION OF DIAMOND DETECTOR DOSE RATE DEPENDENCE WITH LOG OF DIAMOND PDD	
AND LOG OF IC PDD .....	62
FIGURE 3.6: PROFILE SHOWING THE RAW DIAMOND DETECTOR PROFILE AND THE PROFILE WITH DOSE-RATE	
CORRECTION APPLIED (TOPOLNJAK, HEIDE ET AL.) WITH THE DOSE DIFFERENCE (BOTTOM) .....	63
FIGURE 3.7: DIAGRAM SHOWING THE DIRECTION OF THE POSITION OF THE MLC LEAF MOTION WITH	
RESPECT TO THE JAW POSITIONS. NOTE THAT THIS DIAGRAM IS NOT THE VARIAN 120 LEAF MLC	
SYSTEM USED IN THE STUDY. ....	65
FIGURE 3.8: THE END-LEAF OFFSET CONTRIBUTES SIGNIFICANT DOSE IN THE PERPENDICULAR PROFILE	
(LEFT) IF MEASURED WITHOUT ANY OFFSET. THE DETECTOR CAN BE OFFSET SO THAT IT MEASURES	
THE PERPENDICULAR PROFILE AWAY FROM THE CENTRAL AXIS, SO THAT THE OUT-OF-FIELD	
PERPENDICULAR PROFILE DOES NOT MEASURE THE END-LEAF JUNCTION DOSE. ....	67
FIGURE 3.9: THE END-LEAF OFFSET CONTRIBUTES SIGNIFICANT DOSE IN THE PERPENDICULAR PROFILE	
(LEFT) IF MEASURED WITHOUT ANY OFFSET. THE END-LEAF JUNCTION CAN BE OFFSET (RIGHT) SO	
THAT THE OUT-OF-FIELD PERPENDICULAR PROFILE DOES NOT MEASURE THE END-LEAF JUNCTION	
DOSE. ....	67
FIGURE 3.10: <i>CENTRECHECK</i> SOFTWARE INDICATING THAT THE CHAMBER POSITION REQUIRES NO SHIFT TO	
BE IN THE CENTRE WITH THE RADIATION FIELD. ....	70
FIGURE 3.11: FIRST GROUP OF SETTINGS REQUIRED IN TBAScan .....	71
FIGURE 3.12: SECOND GROUP OF SETTINGS IN TBAScan .....	72
FIGURE 3.13: STEP SETTINGS FOR PDD.....	72
FIGURE 3.14: STEP SETTINGS FOR PROFILES .....	73
FIGURE 3.15: SPEED SETTINGS FOR CHAMBER MOVEMENT .....	73
FIGURE 3.16: DELAY TIMES FOR CHAMBER POSITIONS (ZERO WAS SET FOR ALL POSITIONS).....	74
FIGURE 3.17: PROCESSING FUNCTIONS, SHOWING THE SYMMETRISE AND SMOOTH FUNCTION ON THE LEFT	
HAND SIDE OF THE SCREEN .....	74
FIGURE 3.18: THE DEPTH DOSE TAB FOR BEAM MODELLING IN PINNACLE <sup>3</sup> .....	77
FIGURE 3.19: ACTUAL ENERGY SPECTRA USED IN THE STUDY.....	77
FIGURE 3.20: COMPARISON BETWEEN COMPUTED AND MEASURED PDD IN PINNACLE <sup>3</sup> .....	78
FIGURE 3.21: THE BUILD-UP TAB IN THE BEAM MODELLING SECTION IN PINNACLE <sup>3</sup> .....	79
FIGURE 3.22: THE INFELD TAB IN BEAM MODELLING IN PINNACLE <sup>3</sup> .....	80
FIGURE 3.23: THE OUT-OF-FIELD TAB IN THE BEAM MODELLING SECTION IN PINNACLE <sup>3</sup> .....	80
FIGURE 3.24: COMPARISON OF MEASURED AND COMPUTED PROFILES IN PINNACLE <sup>3</sup> .....	82
FIGURE 3.25: THE PHANTOM TAB IN THE BEAM MODELLING SECTION IN PINNACLE <sup>3</sup> .....	82
FIGURE 3.26: THE DVH IN THE PLAN EVALUATION MENU IN PINNACLE <sup>3</sup> .....	86

FIGURE 3.27: ILLUSTRATION OF THE PENUMBRA WIDTH, WHICH IS THE DISTANCE SUBTENDED FROM NORMALISED DOSE VALUES OF 20% AND 80% .....	87
FIGURE 3.28: AN ILLUSTRATION OF THE PERCENTAGE DEPTH DOSE, WITH THE SURFACE DOSE $D_s$ BEING THE SURFACE DOSE, $D_{MAX}$ BEING THE DOSE CORRESPONDING TO MAXIMUM DOSE, AND $D_{EX}$ BEING THE EXIT DOSE. THE REGION BEFORE $D_{MAX}$ IS REFERRED TO AS THE BUILD-UP REGION. FIGURE ADAPTED FROM (IAEA 2005).....	88
<b>FIGURE 3.29: ILLUSTRATION OF THE PROGRAM STRUCTURE USED TO CALCULATE TMR.....</b>	<b>89</b>
FIGURE 4.1: DIAGRAM ILLUSTRATING THE DIMENSIONS OF THE 0.125 CC IONISATION CHAMBER FROM THE MANUFACTURER (PTW-FRIEBURG 2008) .....	93
FIGURE 4.2: DIAGRAM ILLUSTRATING THE DIMENSIONS OF THE PINPOINT DETECTOR FROM THE MANUFACTURER (PTW-FRIEBURG 2008) .....	93
FIGURE 4.3: DIAGRAM ILLUSTRATING THE DIMENSIONS OF THE DIAMOND DETECTOR FROM THE MANUFACTURER (PTW-FRIEBURG 2008). .....	94
FIGURE 4.4: FIGURE SHOWING THE FIRST DERIVATIVE OF A $1 \times 1 \text{ cm}^2$ FIELD AT 10 CM DEPTH .....	95
FIGURE 4.5: FIGURE SHOWING THE FIRST DERIVATIVE OF A $10 \times 10 \text{ cm}^2$ FIELD AT 10 CM DEPTH .....	96
FIGURE 4.6: FIGURE SHOWING THE SECOND DERIVATIVE OF A $1 \times 1 \text{ cm}^2$ FIELD AT 10 CM DEPTH .....	97
FIGURE 4.7: FIGURE SHOWING THE SECOND DERIVATIVE OF A $10 \times 10 \text{ cm}^2$ FIELD AT 10 CM DEPTH .....	97
FIGURE 4.8: PLOT OF THE RATIO OF THE SPATIAL POSITION OF INFLECTION POINT OVER FIELD EDGE WITH SQUARE FIELD SIZE AT 10 CM DEPTH .....	99
FIGURE 4.9: PLOT OF THE NORMALISED DOSE AT INFLECTION POINT FOR EACH SET OF DATA WITH SQUARE FIELD SIZE AT 10 CM DEPTH .....	100
FIGURE 4.10: ENLARGED REGION SHOWING THE INTERSECTION OF THE PROFILES RELATING TO THE IC, PP, AND DD PROFILES.....	101
FIGURE 4.11: FIGURE SHOWING THE DEPENDENCE OF INTERSECTION POINT ON FIELD SIZE .....	102
FIGURE 4.12: PLOT HIGHLIGHTING THE UNDERESTIMATE AREA AND THE OVERESTIMATE AREA IN A PROFILE WITH RELATION TO THE INTERSECTION POINT. ....	104
FIGURE 5.1: ILLUSTRATING THE EXTRAPOLATION PROCEDURE FOR MLC CROSSPLANE $1 \times 1 \text{ cm}^2$ SQUARE FIELD AT 10 CM DEPTH. ....	111
FIGURE 5.2: PLOT OF THE RESULTS OF THE EXTRAPOLATION PROFILE MLC CROSSPLANE $1 \times 1 \text{ cm}^2$ SQUARE FIELD AT 10 CM DEPTH. ....	113
FIGURE 5.3: EXTRAPOLATION PROFILE WITH $R^2$ (DOTTED), COMPARED WITH DATA FROM PROFILES AT A DEPTH OF 10 CM AND FIELD SIZE $1 \times 1 \text{ cm}^2$ (JAW CROSSPLANE DATA). ....	114
FIGURE 5.4: EXTRAPOLATION PROFILE WITH $R^2$ (DOTTED), COMPARED WITH DATA FROM PROFILES AT A DEPTH OF 10 CM AND FIELD SIZE $2 \times 2 \text{ cm}^2$ (JAW CROSSPLANE DATA). ....	114
FIGURE 5.5: EXTRAPOLATION PROFILE WITH $R^2$ (DOTTED), COMPARED WITH DATA FROM PROFILES AT A DEPTH OF 10 CM AND FIELD SIZE $5 \times 5 \text{ cm}^2$ (JAW CROSSPLANE DATA). ....	115
FIGURE 5.6: EXTRAPOLATION PROFILE WITH $R^2$ (DOTTED), COMPARED WITH DATA FROM PROFILES AT A DEPTH OF 10 CM AND FIELD SIZE $10 \times 10 \text{ cm}^2$ (JAW CROSSPLANE DATA). ....	115
FIGURE 5.7: DOSE DIFFERENCE OF EXTRAPOLATION PROFILE WITH IC (DOTTED), COMPARED WITH DATA AT A DEPTH OF 10 CM AND FIELD SIZE $1 \times 1 \text{ cm}^2$ (JAW CROSSPLANE DATA). ....	116
FIGURE 5.8: PLOT OF $R^2$ VERSUS DOSE DIFFERENCE FOR CROSSPLANE JAWS, $1 \times 1 \text{ cm}^2$ AT 10 CM DEPTH. ..	117
FIGURE 5.9: PLOT OF $R^2$ VERSUS DOSE DIFFERENCE FOR INPLANE JAWS, $1 \times 1 \text{ cm}^2$ AT 10 CM DEPTH. ....	118

FIGURE 5.10: PLOT OF $R^2$ VERSUS DOSE DIFFERENCE FOR CROSSPLANE MLC, $1 \times 1 \text{ cm}^2$ AT 10 CM DEPTH.	118
FIGURE 5.11: PLOT OF $R^2$ VERSUS DOSE DIFFERENCE FOR INPLANE MLC, $1 \times 1 \text{ cm}^2$ AT 10 CM DEPTH. ....	119
FIGURE 5.12: SHOWING THE PLOT OF THE COST FUNCTIONS (RHS) WITH THE ZE AND IC PROFILES (LHS) FOR $1 \times 1 \text{ cm}^2$ FIELD DEFINED BY JAW AT A DEPTH OF 10 CM. THE COST FUNCTION IS CALCULATED WITH EQ. 5.1. ....	120
FIGURE 5.13: AVERAGED COST FUNCTION FOR THE IC FOR DOSE POINTS MORE THAN 10% AT A DEPTH OF 10 CM. ....	122
FIGURE 5.14: ZE PROFILE IN THE INPLANE DIRECTION FOR A $1 \times 1 \text{ cm}^2$ FIELD AT A DEPTH OF 10 CM .....	123
FIGURE 5.15: PROFILE ILLUSTRATING THE EFFECT OF EXTRAPOLATING PENUMBRA WITH DETECTOR DIAMETER WITH THE INCLUSION OF A DOSE POINT MEASURED WITH A DETECTOR DIAMETER LESS THAN 1.5 MM (THE DOTTED LINE WAS ADDED TO HIGHLIGHT THE EFFECT OF THE INCLUSION) ADAPTED FROM (PAPPAS, MARIS ET AL. 2006) .....	127
FIGURE 6.1 A DIAGRAM ILLUSTRATING THE CONCEPTS OF THE DETECTOR RESPONSE FUNCTION, THE TRUE PROFILE, AND THE MEASURED PROFILE (CHANG, YIN ET AL. 1996) .....	132
FIGURE 6.2: FIGURE SHOWING THE DECONVOLUTION OF RAW IC DATA AND THE DECONVOLUTION OF A GAUSSIAN FIT OF IC DATA .....	135
FIGURE 6.3: GAUSSIAN CURVE FIT FOR $1 \times 1 \text{ cm}^2$ AT 10 CM DEPTH .....	137
FIGURE 6.4: GAUSSIAN CURVE FIT FOR $2 \times 2 \text{ cm}^2$ CURVE AT 10 CM DEPTH .....	137
FIGURE 6.5: GAUSSIAN CURVE FIT FOR $5 \times 5 \text{ cm}^2$ CURVE AT 10 CM DEPTH .....	138
FIGURE 6.6: FIGURE SHOWING THE PLOT OF THE KERNEL FUNCTIONS .....	139
FIGURE 6.7: DECONVOLUTION OF IC WITH VARIOUS KERNELS COMPARED WITH ZE FOR A $1 \times 1 \text{ cm}^2$ FIELD AT 10 CM DEPTH (JAW CROSSPLANE) .....	141
FIGURE 6.8: DECONVOLUTION OF PP WITH VARIOUS KERNELS COMPARED WITH ZE FOR A $1 \times 1 \text{ cm}^2$ FIELD AT 10 CM DEPTH (JAW CROSSPLANE) .....	142
FIGURE 6.9: DECONVOLUTION OF DD WITH VARIOUS KERNELS COMPARED WITH ZE FOR A $1 \times 1 \text{ cm}^2$ FIELD AT 10 CM DEPTH (JAW CROSSPLANE) .....	143
FIGURE 7.1: PLOT OF PENUMBRAL VARIATION OVER FIELD SIZES (10 CM DEPTH) .....	151
FIGURE 7.2: MEASURED FIELD SIZE VARIATION OVER SET FIELD SIZE (OVER DEPTHS 1.5 TO 20 CM AND SET FIELD SIZE $1 \times 1$ TO $10 \times 10 \text{ cm}^2$ ) .....	154
FIGURE 7.3: MEASURED FIELD SIZE VARIATION OVER DEPTH ( $1 \times 1 \text{ cm}^2$ FIELD SIZE) .....	155
FIGURE 7.4: DOSE DIFFERENCE VARIATION OVER FIELD SIZE (10 CM DEPTH); PLOT OF THE MAXIMUM DOSE DIFFERENCE AS A PERCENTAGE OVER FIELD SIZES. THE Y-AXIS IS CALCULATED USING EQUATION 7.1. ....	158
FIGURE 7.5: DOSE DIFFERENCE VARIATION OVER DEPTH ( $1 \times 1 \text{ cm}^2$ FIELD SIZE); PLOT OF THE MAXIMUM DOSE DIFFERENCE AS A PERCENTAGE OVER DEPTH. ....	159
FIGURE 7.6: PLOT OF THE SUMMED OF THE OVERESTIMATE AND UNDERESTIMATE AS A PERCENTAGE OF THE TOTAL SUMMED DOSE IN THE PROFILE WITH FIELD SIZE. THE SUMMED(OVERESTIMATE) IS CALCULATED USING EQ. 7.5, SUMMED(UNDERESTIMATE) USES EQ. 7.6, AND OVERALL CHANGE USES EQ. 7.7. ....	160
FIGURE 7.7: PLOT OF THE SUMMED OF THE OVERESTIMATE AND UNDERESTIMATE AS A PERCENTAGE OF THE TOTAL SUMMED DOSE IN THE PROFILE WITH DEPTH. THE SUMMED(OVERESTIMATE) IS CALCULATED USING EQ. 7.5, SUMMED(UNDERESTIMATE) USES EQ. 7.6, AND OVERALL CHANGE USES EQ. 7.7. ..	162

FIGURE 7.8: PLOT OF THE RATIO OF THE SUMMED OVERESTIMATE AND UNDERESTIMATE IN THE PROFILE WITH FIELD SIZE. ....	163
FIGURE 8.1: FIGURE ILLUSTRATING A PLOT WHICH INCLUDES BOTH THE EFFECTS OF PENUMBRAL INCREASE DUE TO FIELD SIZE (ILLUSTRATED WITH CLOSED CIRCLES $1 \times 1 \text{ cm}^2$ , OPEN CIRCLES $2 \times 2 \text{ cm}^2$ , TRIANGLES $5 \times 5 \text{ cm}^2$ , AND STARS $10 \times 10 \text{ cm}^2$ ) AND DEPTH (ILLUSTRATED WITH RED FOR DEPTH 1.5 CM, BLACK FOR DEPTH 5.0 CM, GREEN FOR DEPTH 10.0 CM, AND BLUE FOR DEPTH 20.0 CM).....	175
FIGURE 8.2: PLOT SHOWING THE RELATIONSHIP BETWEEN THE CHANGE IN PENUMBRA SIZE DUE TO DETECTOR DIAMETER AND THE MEASURED ZE PENUMBRA FOR THE JAW CROSSPLANE DATA.....	176
FIGURE 8.3 PLOT SHOWING THE RELATIONSHIP BETWEEN THE CHANGE IN PENUMBRA SIZE DUE TO DETECTOR DIAMETER AND THE MEASURED ZE PENUMBRA FOR THE MLC CROSSPLANE .....	177
FIGURE 8.4: DIAGRAM ILLUSTRATING THE CORRELATION BETWEEN THE INCREASE IN MEASURED PENUMBRA FROM ZE PENUMBRA WITH DETECTOR DIAMETER (SEE EQUATION 8.1) .....	178
FIGURE 8.5: PLOT OF THE RELATIONSHIP BETWEEN THE LINEAR COEFFICIENT M1 AND THE ZE PENUMBRA FOR THE JAW CROSSPLANE DATA .....	179
FIGURE 8.6: PLOT OF THE RELATIONSHIP BETWEEN THE LINEAR COEFFICIENT M1 AND THE ZE PENUMBRA FOR THE MLC CROSSPLANE DATA .....	179
FIGURE 8.7: PLOT OF THE SIMULATED ZE PENUMBRA CALCULATED BY THE NON-LINEAR ZE PENUMBRA EQUATION FOR AN ARBITRARY DETECTOR DIAMETER .....	182
FIGURE 8.8: PLOT SHOWING THE DEVIATION FROM THE ZE PENUMBRA WITH THE IC DATA WITH AND WITHOUT THE CORRECTION MADE WITH THE NON-LINEAR PENUMBRA EQUATION WITH THE JAW CROSSPLANE DATA .....	183
FIGURE 8.9: PLOT SHOWING THE DEVIATION FROM THE ZE PENUMBRA WITH THE PP DATA WITH AND WITHOUT THE CORRECTION MADE WITH THE NON-LINEAR PENUMBRA EQUATION WITH THE JAW CROSSPLANE DATA .....	183
FIGURE 8.10: PLOT SHOWING THE DEVIATION FROM THE ZE PENUMBRA WITH THE DD DATA WITH AND WITHOUT THE CORRECTION MADE WITH THE NON-LINEAR PENUMBRA EQUATION WITH THE JAW CROSSPLANE DATA .....	184
FIGURE 8.11: PLOT SHOWING THE DEVIATION FROM THE ZE PENUMBRA WITH THE IC DATA WITH AND WITHOUT THE CORRECTION MADE WITH THE NON-LINEAR PENUMBRA EQUATION WITH THE MLC CROSSPLANE DATA .....	186
FIGURE 8.12: PLOT SHOWING THE DEVIATION FROM THE ZE PENUMBRA WITH THE PP DATA WITH AND WITHOUT THE CORRECTION MADE WITH THE NON-LINEAR PENUMBRA EQUATION WITH THE MLC CROSSPLANE DATA .....	187
FIGURE 8.13: PLOT SHOWING THE DEVIATION FROM THE ZE PENUMBRA WITH THE DD DATA WITH AND WITHOUT THE CORRECTION MADE WITH THE NON-LINEAR PENUMBRA EQUATION WITH THE MLC CROSSPLANE DATA .....	187
FIGURE 8.14: THE EFFECT OF VARIOUS IC15 LINE SPREAD FUNCTIONS ON THE BROADENING OF 20%-80% PENUMBRA AS MODELLED BY THE DECONVOLUTION MODEL INVOLVING THE ELLIPTIC AND GAUSSIAN KERNEL FUNCTION (VAN'T.VELD, LUJIK ET AL. 2001).....	190
FIGURE 9.1: PLOT ILLUSTRATING THE RELIABILITY OF THE RELATIONSHIP BETWEEN THE PINNACLE MODELLED PENUMBRA AND THE PINNACLE SOURCE SIZE. ....	197

FIGURE 9.2: THE CALCULATED PINNACLE SOURCE SIZE (MM) WITH VARIOUS DATASETS OVER DEPTH AT A FIELD SIZE OF $1 \times 1 \text{ cm}^2$ .....	199
FIGURE 9.3: THE CALCULATED PINNACLE SOURCE SIZE (MM) WITH VARIOUS DATASETS OVER VARIOUS FIELD SIZES AT A DEPTH OF 1.5 CM. ....	201
FIGURE 9.4: FIGURE ILLUSTRATING THE RELATIONSHIP BETWEEN THE ZE PENUMBRA FOR THE ZE AND THE MEASURED DETECTOR DATASET. ....	202
FIGURE 9.5: FIGURE ILLUSTRATING THE RELATIONSHIP BETWEEN THE ZE PENUMBRA FOR THE ZE AND THE NON-LINEAR PENUMBRA CORRECTED DETECTOR DATASET. ....	203
FIGURE 9.6: FIGURE SHOWING THE DIFFERENCE BETWEEN THE CALCULATED PINNACLE SOURCE SIZE USING FINITE DETECTORS AND THE ZE CALCULATED PINNACLE SOURCE SIZE MODELLED TO MATCH ZE PENUMBRA PROFILES. ....	204
FIGURE 9.7: COMPARISON OF CALCULATED SOURCE SIZE BASED ON GEOMETRIC PENUMBRA AND MODELLED SOURCE SIZE BASED ON RTPS MODEL OF PENUMBRA .....	205
FIGURE 10.1: PINNACLE ISODOSE DISTRIBUTION SHOWING THE BEAM GEOMETRY USED IN THE PLAN 4FS1 .....	217
FIGURE 10.2: PLOT SHOWING THE DIFFERENCE IN ISODOSE DISTRIBUTION FOR ONE $1 \times 1 \text{ cm}^2$ FIELD BETWEEN THE 0.4 MM SOURCE SIZE MODEL (TOP) AND THE 2.4 MM SOURCE SIZE MODEL (BOTTOM) USED IN THE PLAN 4FS10.....	218
FIGURE 10.3 PLOT SHOWING THE ISODOSE DIFFERENCE PLOT FOR A SINGLE FIELD (GANTRY 0), WHERE EACH POINT WAS CALCULATED BY ISODOSE POINT (2.4 MM MODEL) MINUS ISODOSE POINT (0.8 MM MODEL) .....	219
FIGURE 10.4: PLOT SHOWING THE DIFFERENCE IN ISODOSE DISTRIBUTION FOR 4 $1 \times 1 \text{ cm}^2$ FIELDS BETWEEN THE 0.4 MM SOURCE SIZE MODEL (TOP) AND THE 2.4 MM SOURCE SIZE MODEL (BOTTOM) USED IN THE PLAN 4FS10.....	219
FIGURE 10.5: PLOT SHOWING THE ISODOSE DIFFERENCE PLOT FOR COMBINED 4 FIELDS, WHERE EACH POINT WAS CALCULATED BY ISODOSE POINT (2.4 MM MODEL) MINUS ISODOSE POINT (0.8 MM MODEL) ....	220
FIGURE 10.6: PROFILE ACROSS THE ROWS IN FIGURE 10.5 AT $Y=0$ FOR COMBINED BEAMS.....	220
FIGURE 10.7: DOSE ANALYSIS IN TERMS OF SUMMATION OF 2D DOSE IN A SINGLE $1 \times 1 \text{ cm}^2$ FIELD .....	221
FIGURE 10.8: DOSE ANALYSIS IN TERMS OF SUMMATION OF 2D DOSE IN A FOUR $1 \times 1 \text{ cm}^2$ FIELD ARRANGEMENT.....	222
FIGURE 10.9: PINNACLE ISODOSE DISTRIBUTION SHOWING THE BEAM GEOMETRY USED IN THE PLAN 2FS1A .....	223
FIGURE 10.10: PLOT SHOWING THE ISODOSE DIFFERENCE PLOT, AT GANTRY 0 FOR TWO SINGLE FIELDS (GANTRY 0), WHERE EACH POINT WAS CALCULATED BY ISODOSE POINT (2.4 MM MODEL) MINUS ISODOSE POINT (0.8 MM MODEL).....	224
FIGURE 10.11: PLOT SHOWING THE DIFFERENCE IN ISODOSE DISTRIBUTION FOR ONE $2 \times 1$ (ABUTTED) $\text{cm}^2$ FIELD BETWEEN THE 0.4 MM SOURCE SIZE MODEL (TOP) AND THE 2.4 MM SOURCE SIZE MODEL (BOTTOM) .....	224
FIGURE 10.12 ISODOSE DIFFERENCE. NORMALISED ISODOSES 24 MINUS NORMALIZED ISODOSES 08, COMBINED FIELDS.....	225
FIGURE 10.13 PROFILE WITH DATA FROM ROWS ALONG $Y=2.45 \text{ cm}$ (HIGHEST DOSE REGION) SHOWING DIFFERENT SOURCE SIZE FOR COMBINED BEAMS.....	225

FIGURE 10.14: PINNACLE ISODOSE DISTRIBUTION SHOWING THE BEAM GEOMETRY USED IN THE PLAN 4FS10	226
FIGURE 10.15: PLOT SHOWING THE DIFFERENCE IN ISODOSE DISTRIBUTION FOR ONE $10 \times 10 \text{ cm}^2$ FIELD BETWEEN THE 0.4 MM SOURCE SIZE MODEL (TOP) AND THE 2.4 MM SOURCE SIZE MODEL (BOTTOM) USED IN THE PLAN 4FS10	227
FIGURE 10.16: PLOT SHOWING THE ISODOSE DIFFERENCE PLOT, AT GANTRY 0 FOR TWO SINGLE FIELDS (GANTRY 0), WHERE EACH POINT WAS CALCULATED BY ISODOSE POINT (2.4 MM MODEL) MINUS ISODOSE POINT (0.8 MM MODEL)	228
FIGURE 10.17: PLOT SHOWING THE ISODOSE DIFFERENCE PLOT, AT GANTRY 0 FOR FOUR SINGLE FIELD THAT ARE $10 \times 10 \text{ cm}^2$ , WHERE EACH POINT WAS CALCULATED BY ISODOSE POINT (2.4 MM MODEL) MINUS ISODOSE POINT (0.8 MM MODEL)	228
FIGURE 10.18: PLOT SHOWING THE ISODOSE DIFFERENCE PLOT, AT GANTRY 0 FOR FOUR SINGLE FIELDS THAT ARE $10 \times 10 \text{ cm}^2$ (GANTRY 0), WHERE EACH POINT WAS CALCULATED BY ISODOSE POINT (2.4 MM MODEL) MINUS ISODOSE POINT (0.8 MM MODEL)	229
FIGURE 10.19: PROFILE FROM ROW DATA ALONG $Y=0$ (CENTRAL REGION) SHOWING DIFFERENT SOURCE SIZE FOR COMBINED BEAMS	229
FIGURE 10.20: DOSE ANALYSIS IN TERMS OF SUMMATION OF 2D DOSE IN A SINGLE $10 \times 10 \text{ cm}^2$ FIELD	230
FIGURE 10.21: DOSE ANALYSIS IN TERMS OF SUMMATION OF 2D DOSE IN A FOUR $10 \times 10 \text{ cm}^2$ FIELD ARRANGEMENT	230
FIGURE 10.22: PINNACLE ISODOSE DISTRIBUTION SHOWING THE BEAM GEOMETRY USED IN THE PLAN PROST	231
FIGURE 10.23: PLOT SHOWING THE DIFFERENCE IN ISODOSE DISTRIBUTION FOR AN OBLIQUE $10 \times 10 \text{ cm}^2$ FIELD BETWEEN THE 0.4 MM SOURCE SIZE MODEL (TOP) AND THE 2.4 MM SOURCE SIZE MODEL (BOTTOM) USED IN THE PLAN 4FS10	232
FIGURE 10.24: PLOT SHOWING THE ISODOSE DIFFERENCE PLOT, AT GANTRY 0 FOR THE OBLIQUE FIELD, WHERE EACH POINT WAS CALCULATED BY ISODOSE POINT (2.4 MM MODEL) MINUS ISODOSE POINT (0.8 MM MODEL)	233
FIGURE 10.25: PLOT SHOWING THE CONTOUR PLOTS FOR THE TWO SOURCE SIZE SETTING IN THE PROSTATE PLAN, WHERE EACH POINT WAS CALCULATED BY ISODOSE POINT (2.4 MM MODEL) MINUS ISODOSE POINT (0.8 MM MODEL)	233
FIGURE 10.26: PLOT SHOWING THE ISODOSE DIFFERENCE PLOT, FOR FOUR IN THE PROSTATE PLAN, WHERE EACH POINT WAS CALCULATED BY ISODOSE POINT (2.4 MM MODEL) MINUS ISODOSE POINT (0.8 MM MODEL)	234
FIGURE 10.27: PLOT OF THE DEPENDENCE OF CHANGE OF THE MEAN DOSE AS A PERCENTAGE OF THE MEAN DOSE OF THE SOURCE SIZE 0.8 MM WITH SOURCE SIZE	235
FIGURE C.1: THE END-LEAF OFFSET CONTRIBUTES SIGNIFICANT DOSE IN THE PERPENDICULAR PROFILE (LEFT) IF MEASURED WITHOUT ANY OFFSET. THE END-LEAF JUNCTION CAN BE OFFSET (RIGHT) SO THAT THE OUT-OF-FIELD PERPENDICULAR PROFILE DOES NOT MEASURE THE END-LEAF JUNCTION DOSE	261
FIGURE C.2: CONSIDERATION OF THE EFFECTIVE DISTANCE OF THE CENTRAL AXIS TO THE CLOSEST DOSE POINT IN THE LEAF-END DOSE REGION WITH REGARDS TO PHANTOM SCATTER AT 100 CM SAD. THE MLC LEAF-END OFFSET IS ALSO SHOWN HERE	261

FIGURE C.3: EFFECT OF END-LEAF OFFSET ON THE DOSE AT DMAX. THE READING ASSOCIATED WITH AN END-LEAF OFFSET OF 0 CM WAS THE HIGHEST AND WAS USED TO COMPARE WITH THE OTHER READINGS. ....	262
FIGURE C.4: A NORMALISED PERPENDICULAR PROFILE SHOWING THE EFFECT OF THE LEAF-END OFFSET ON THE OUT OF FIELD DOSE, THE FIELD EDGE, AND THE PENUMBRA.....	263
FIGURE C.5: PLOT OF THE LEAF END JUNCTION PROFILE AT A DEPTH OF 1.5 CM FOR A CLOSED MLC FIELD WITH VARIOUS LEAF END OFFSETS .....	264
FIGURE D.1: PLOT OF TPR (20,10) WITH SQUARE FIELD SIZE DEFINED BY THE JAW AND MLC AND MEASURED WITH IC, PP, AND DD. ....	269
FIGURE D.2: VARIATION OF THE DIAMETER ASSOCIATED WITH LATERAL ELECTRON EQUILIBRIUM AS CALCULATED FROM $TPR_{(20,10)}$ COMPARED WITH THE INCREASE OF SQUARE FIELD SIZE (RED). THE INTERSECTION SHOWS THE MINIMUM FIELD SIZE WHERE THERE IS LEE FOR THE CASE OF JAWS AND MLCS.....	270
FIGURE E.1: FIGURE SHOWING THE DIMENSIONS OF THE MODEL USED.....	274
FIGURE E.2: ILLUSTRATION OF THE OUT OF FIELD RELATIVE TO THE CENTRAL AXIS READING AS A % WITH INCREASING SQUARE FIELD SIZE FOR THE CASE OF MLC AND JAW WITH DIFFERENT DETECTOR READINGS. DATA ANALYSED WITH A DEPTH OF 10 CM. ....	275
FIGURE E.3: RESULTS OF MODELLED NORMAL DOSE OVER TUMOUR DOSE FOR JAW SETTINGS. SP1 CONSIDERS A NORMAL TISSUE VOLUME 1 CM AROUND THE TUMOUR VOLUME. ....	276
FIGURE E.4: RESULTS OF MODELLED NORMAL DOSE OVER TUMOUR DOSE FOR MLC SETTINGS. SP1 CONSIDERS A NORMAL TISSUE VOLUME 1 CM AROUND THE TUMOUR VOLUME. ....	276
FIGURE G.1: VARIATION OF BEAM QUALITY ACROSS THE PROFILE FOR A $1 \times 1 \text{ cm}^2$ FIELD.....	284
FIGURE G.2: VARIATION OF BEAM QUALITY ACROSS THE PROFILE FOR A $5 \times 5 \text{ cm}^2$ FIELD .....	285
FIGURE G.3: VARIATION OF BEAM QUALITY ACROSS THE PROFILE FOR A $10 \times 10 \text{ cm}^2$ FIELD.....	286
FIGURE G.4: THE BEAM QUALITY VARIATION WITH FIELD SIZE (BLACK). THE CHANGE IN BEAM QUALITY ACROSS THE PROFILE IS ALSO PLOTTED (RED) WITH FIELD SIZE. ....	286



## LIST OF TABLES

TABLE 2.1: DATA ILLUSTRATING THE MINIMUM BEAM DIAMETER CORRESPONDING TO LATERAL ELECTRON EQUILIBRIUM (LEE) FOR DIFFERENT LINAC BEAM ENERGIES, ADAPTED FROM (LI, SOUBRA ET AL. 1995) .....	23
TABLE 2.2: A COMPARISON OF SELECTED FEATURES OF A SAMPLE OF DETECTORS.....	35
TABLE 3.1: SPECIFICATIONS FOR THE 0.125 CC IONISATION CHAMBER USED IN THIS STUDY (PTW-FRIEBURG 2008) .....	58
TABLE 3.2: SPECIFICATIONS FOR THE PINPOINT CHAMBER USED IN THIS STUDY (PTW-FRIEBURG 2008) ...	59
TABLE 3.3: SPECIFICATIONS FOR THE DIAMOND DETECTOR USED IN THIS STUDY (PTW-FRIEBURG 2008) .	60
TABLE 3.4: ORIENTATION OF LINEAR ACCELERATOR TO ILLUSTRATE THE DIFFERENT IN NAMING CONVENTIONS AS WELL AS COMMONLY USED TERMS.....	64
TABLE 3.5: SETTINGS USED FOR JAW DATA ACQUISITION.....	68
TABLE 3.6: SETTINGS USED FOR MLC DATA ACQUISITION .....	69
TABLE 3.7: ILLUSTRATION OF THE DATA FORMAT REQUIRED BY PINNACLE <sup>3</sup> .....	75
TABLE 3.8: INFIELD TAB PARAMETERS USED .....	79
TABLE 3.9: OUT-OF-FIELD PARAMETERS USED .....	81
TABLE 3.10: THE PINNACLE <sup>3</sup> DOSE MAP FORMAT REQUIRED. THE FILE ENDS WITH “PTS”. .....	84
TABLE 3.11: THE FILE FORMAT OF THE EXPORTED PINNACLE <sup>3</sup> PLANAR DOSE DISTRIBUTION.....	85
TABLE 3.12 TABULATED DATA OF PARAMETERS USED IN EXAMPLE CALCULATION OF TPR FROM PDD AND PSF.....	89
TABLE 4.1: TABULATED VOLUME, ACTIVE SIZE, AND PHYSICAL SIZE FOR DETECTORS USED (PTW-FRIEBURG 2008) .....	92
TABLE 4.2: TABULATED DATA SHOWING THE SPATIAL POSITION OF THE INFLECTION POINT, THE FIELD EDGE, AND THE RATIO OF THE TWO VALUES .....	98
TABLE 4.3: TABULATED DATA SHOWING THE AVERAGE DOSE AT THE INTERSECTION POINT AND THE DEVIATION FROM EXPECTED INFLECTION POINT <i>THE DATA IS DERIVED FROM A DEPTH OF 10 CM AT VARIOUS FIELD SIZES.</i> .....	103
TABLE 4.4: TABULATED DATA SHOWING THE EFFECT OF DETECTOR VOLUME ON DOSE WITH RESPECT TO THE REGIONS IN THE PROFILE. ....	105
TABLE 6.1: A SELECTION OF MODELS OF KERNELS USED FOR DECONVOLUTION. ....	133
TABLE 6.2: EQUATIONS RELATING TO THE DIFFERENT ORDERS OF GAUSSIAN FUNCTION, AND MAXIMUM DIFFERENCES FROM MEASURED DATA. ....	136
TABLE 6.3: NOTATION USED IN FIGURES 6.7, 6.8, 6.9. ....	140
TABLE 7.1: OVERESTIMATE OF THE PENUMBRA FROM ZE PENUMBRA IN MM WITH VARIATION WITH FIELD SIZE.....	151
TABLE 7.2: PENUMBRAL VARIATION OVER DEPTHS (1x1 cm <sup>2</sup> FIELD SIZE); PLOT SHOWING THE DEPENDENCE OF THE DIFFERENCE IN PENUMBRA MEASUREMENT FROM ZE PENUMBRA WITH DEPTH. ....	152
TABLE 7.3: OVERESTIMATE OF THE PENUMBRA FROM ZE PENUMBRA IN MM WITH VARIATION WITH DEPTH. ....	153
TABLE 7.4: OVERESTIMATE OF THE FIELD SIZE FROM ZE FIELD SIZE IN MM WITH FIELD SIZE (SEE FIG. 7.2) .....	155

TABLE 7.5: OVERESTIMATE OF THE FIELD SIZE FROM ZE FIELD SIZE IN MM WITH DEPTH (SEE FIG. 7.3) ....	156
TABLE 7.6: MAXIMUM DOSE DIFFERENCE ALONG THE PROFILE OVER FIELD SIZE (SEE FIG. 7.4) .....	159
TABLE 7.7: MAXIMUM DOSE DIFFERENCE ACROSS THE PROFILE WITH DEPTH (SEE FIG. 7.5) .....	160
TABLE 7.8: TABULATED DATA OF OVERESTIMATES AND UNDERESTIMATES OF PROFILE WITH FIELD SIZE (SEE FIG. 7.6) .....	161
TABLE 7.9: TABULATED DATA OF OVERESTIMATES AND UNDERESTIMATES OF PROFILE WITH DEPTH (SEE FIG. 7.7) .....	162
TABLE 7.10: TABULATED DATA OF THE RATIO OF OVERESTIMATES AND UNDERESTIMATES OF PROFILE WITH FIELD SIZE. THE FIELD SIZE OF $2.3 \times 2.3 \text{ cm}^2$ WAS INTERPOLATED FROM THE GRAPH IN FIGURE 7.8. .	163
TABLE 7.11: SUMMARY OF THE DOSE ANALYSIS WITH COMMENTS ON THE CLINICAL IMPLICATIONS OVER FIELD SIZES. ....	169
TABLE 8.1: EXPERIMENTALLY DETERMINED COEFFICIENTS FOR THE NON-LINEAR ZE PENUMBRA EQUATION .....	181
TABLE 8.2: TABULATED DATA SHOWING A SUMMARY OF THE CHANGE IN ERRORS IN TERMS OF VARIATION OF PENUMBRA FROM THE ZE PENUMBRA DUE TO THE APPLICATION OF THE NON-LINEAR PENUMBRA EQUATION FOR THE JAW CROSSPLANE DATA .....	185
TABLE 8.3: TABULATED DATA SHOWING A SUMMARY OF THE CHANGE IN ERRORS IN TERMS OF VARIATION OF PENUMBRA FROM THE ZE PENUMBRA DUE TO THE APPLICATION OF THE NON-LINEAR PENUMBRA EQUATION FOR THE MLC CROSSPLANE DATA .....	188
TABLE 9.1: THE VARIATION OF THE PINNACLE SOURCE SIZE AND THE PINNACLE MODELLED PENUMBRA IN MM .....	196
TABLE 9.2: COEFFICIENTS OF THE POLYNOMIAL RELATIONSHIP BETWEEN THE PINNACLE SOURCE SIZE AND PINNACLE MODELLED PENUMBRA AT VARIOUS FIELD SIZES AND DEPTHS (FOR JAW CROSSPLANE DATA) .....	198
TABLE 9.3: AVERAGED PINNACLE SOURCE SIZES, VARIATION OF SOURCE SIZE WITH DEPTH, AND DEVIATION FROM THE ZE SOURCE SIZE FOR VARIOUS DATASETS OVER DEPTHS AT A FIELD SIZE OF $1 \times 1$ $\text{cm}^2$ (SEE FIGURE 9.2) .....	200
TABLE 9.4: AVERAGED PINNACLE SOURCE SIZES, VARIATION OF SOURCE SIZE WITH DEPTH, AND DEVIATION FROM THE ZE SOURCE SIZE FOR VARIOUS DATASETS OVER VARIOUS FIELD SIZES AT A DEPTH OF 1.5 CM (SEE FIGURE 9.3) .....	201
TABLE 9.5: TABULATED DATA SHOWING THE AVERAGE DIFFERENCE FROM CALCULATED SOURCE SIZE WITH THE ZE CALCULATED SOURCE SIZE OVER FIELD SIZE OF $1 \times 1 \text{ cm}^2$ AND DEPTH 1.5 CM. THE ZE SOURCE SIZE WAS 0.9 MM. ....	206
TABLE 9.6: MODELLING OF THE SENSITIVE DIAMETER OF PTW DETECTORS WITH MEASURED PENUMBRA IN COLUMN 3 (SEE EQUATION 8.5) AND THE PINNACLE RTPS SOURCE SIZE IN COLUMN 4(SEE EQUATION 9.1) AT A FIELD SIZE OF $1 \times 1 \text{ cm}^2$ AND DEPTH 1.5 CM. ....	210
TABLE 10.1: PINNACLE PARAMETERS USED IN THE PLAN 4 FIELD $1 \times 1 \text{ cm}^2$ (4FS1) .....	215
TABLE 10.2: PINNACLE PARAMETERS USED IN THE PLAN 2 FIELD $1 \times 1 \text{ cm}^2$ ABUTTED (2FSA) .....	215
TABLE 10.3: PINNACLE PARAMETERS USED IN THE PLAN 4 FIELD $10 \times 10 \text{ cm}^2$ (4FS10) .....	216
TABLE 10.4: PINNACLE PARAMETERS USED IN THE PLAN PROSTATE .....	216
TABLE 10.5: DOSE VOLUME HISTOGRAM DATA SHOWING THE MEAN DOSE OF VARIOUS STRUCTURES AS A FUNCTION OF SOURCE SIZE .....	234

TABLE 10.6: TABULATED RESULTS DETAILING THE MAXIMUM POINT DIFFERENCES AND SUMMED OVERALL CHANGE FOR THE $1 \times 1 \text{ cm}^2$ AND $10 \times 10 \text{ cm}^2$ FIELD SIZE BEAMS OVER A SINGLE FIELD AND FOUR FIELD ARRANGEMENT BETWEEN THE ZE MODEL AND THE IC MODEL .....	238
TABLE A.1: SETTINGS USED FOR THE INVESTIGATION OF JAW-MLC SEPARATION .....	253
TABLE C.1: TABLE SHOWING THE FWHM (FIELD SIZE) IN CM WITH VARIATION WITH DEPTH AND LEAF-END OFFSET FOR A MLC FIELD SIZE OF $1 \times 1 \text{ cm}^2$ , JAW SETTING OF $30 \times 30 \text{ cm}^2$ .....	263
TABLE F.1: FILE FORMAT OF THE MCC FORMAT USED WITH MEPHYSTO $\text{mc}^2$ (PART 1/2) .....	280
TABLE F.2 FORMAT OF THE MCC FORMAT USED WITH MEPHYSTO $\text{mc}^2$ (PART 2/2) .....	281
TABLE H.1: ANONYMOUS RESULTS FROM THE SOURCE SIZE SURVEY FOR THE PINNACLE RTPS (PTO) .....	289
TABLE I.1: DECONVOLUTION CODE USED IN MATLAB FOR THE THESIS (PTO) .....	295
TABLE J.1: CODE FOR CREATION OF THE PLANAR DOSE FILE FOR THE PINNACLE RTPS .....	298

## LIST OF ABBREVIATIONS

Abbreviation	Meaning
3DCRT	Three-dimensional conformal radiation therapy
CPE	Charged particle equilibrium
d(DD)	Deconvolved DD data
d(IC)	Deconvolved IC data
d(PP)	Deconvolved PP data
DD	Diamond Detector
DDC	DD penumbra with non-linear penumbral correction (see Chapter 8)
DVH	Dose volume histogram
IC	0.125 cc Ionisation Chamber
ICC	IC penumbra with non-linear penumbral correction (see Chapter 8)
IMRT	Intensity modulated radiation therapy
LEE	Lateral electron equilibrium
MLC	Multi-leaf collimator
PDD	Percentage depth dose
PP	Pinpoint Chamber
PPC	PP penumbra with non-linear penumbral correction (see Chapter 8)
PTV	Planning target volume
QA	Quality assurance
RTPS	Radiotherapy treatment planning system
TPR	Tissue phantom ratio
ZE	Virtual zero extrapolated volume data

## **Abstract**

*Introduction* With the adoption of technologies such as stereotactic radiosurgery in the treatment of cancer, there is an increasing trend towards smaller field sizes where the importance of accurate penumbral measurements is critical. Small segments are also common in intensity modulated radiation therapy deliveries; hence accurate dose assessment at the edge of multi-leaf collimated segmented fields is also paramount.

Clinically used detectors have significant detector volumes that contribute to measurement of wider penumbral dose profiles than the beam produces. This overestimate of penumbral width in turn has an impact on the radiotherapy treatment planning modelled dose distributions used for patient treatment. This is because the penumbra broadening in the dose profile affects the source size parameter used in radiotherapy treatment planning system. In this thesis, the extent of penumbral broadening was quantified and methods to produce data with effectively zero detector volumes were investigated. This data was used to calculate a source size for the computer model to best match the measured data.

*Methods* Data was measured for a 6 MV beam (Varian Clinac 600C) using a diamond detector, a pinpoint detector, and a 0.125 cc ionisation chamber. Extrapolation and deconvolution techniques were used to calculate zero detector volume data. The extrapolation technique was studied in detail and a new verification technique, which involved  $R^2$  and dose differences, was developed to calculate the fit and errors associated with the extrapolation method. The amount of penumbral broadening and source size overestimation in Pinnacle decreased with decreasing detector diameter.

*Results* In this study, penumbral broadening of up to +1.8 mm (80%-20% penumbra) due to the detector volume effect was found to occur across both large and small field sizes and this resulted in overestimations in the source size parameter in the Pinnacle radiotherapy treatment planning system by +1.2 mm for the 0.125cc ionisation chamber (from the zero detector source size of 0.9 mm).

The effect of source size overestimation in Pinnacle was studied by the calculation of dose distributions with the virtual zero detector dataset and the 0.125 cc ionisation chamber dataset.

The point in the middle of the field had minimal change but there were changes in the dose distribution which were due to a summation of penumbral perturbations of each beam. It was found that for large field sizes ( $\sim 10 \times 10 \text{ cm}^2$ ) the summed doses in the treatment region were underestimated by approximately 0.5%. For small field sizes

( $1 \times 1 \text{ cm}^2$ ) summed dose in the treatment region was overestimated by approximately 3.5% while over the whole region there was an overestimation of approximately 11%. For the case of a 3DCRT prostate plan, changes in dose were underestimated by to 1% for volumes typical of the PTV and overestimated by up to +1.5% for volumes typical of organs at risk.

Equations were derived that produced agreeable links between the detector volume and the penumbral width as well as the penumbral width and the source size parameter in Pinnacle. The coefficients required in these equations were calculated from datasets obtained from the measurement of dose profiles by physical detectors and the calculation of dose profiles in the treatment planning system respectively. The use of these equations could be used to estimate and/or correct for the detector volume effect on the source size parameter in the treatment planning system with a minimum of beam measurement time. However, further investigations are required to verify this over a wide range of conditions such as beam energy and collimator design.

The 1D dose profiles measured with different detectors were analysed in terms of intersection point and inflection point. The results indicated that there were significant deviations of both these points from a normalised dose of 50% with small field sizes. There was an overestimate of the radiation field size (50%) by 0.8 mm measured with the 0.125cc ionisation chamber at the field size of  $1 \times 1 \text{ cm}^2$  but at other field sizes measured the radiation field size was within  $\pm 0.2 \text{ mm}$ . The intersection point determined the spatial location of overestimation and underestimation of point and summed dose. The overall summed dose was found to be unaffected by the detector volume effect at a field size of  $2.3 \times 2.3 \text{ cm}^2$ , which was similar to the minimum field size for lateral electron equilibrium ( $2.6 \times 2.6 \text{ cm}^2$ ).

*Conclusions-* The results of a survey of different radiotherapy institutions indicated that approximately half of measurements done for use in modelling the Pinnacle radiation treatment planning system involved the use of ionisation chambers (approximately  $0.1 \text{ cm}^3$ ). In this study, it was demonstrated that (1) the detector volume effect is significant as matching the model to broad penumbra overestimates the virtual source size parameter by the order of +1 mm in Pinnacle; (2) that the effect on dose distributions for single fields in the penumbra the dose may be different by 1-10% compared with zero detector profile matched data (3) that corrections to the detector volume can be made with a new single detector technique combined with a predictive equation. This makes the correction more feasible with consideration to time constraints

## Acknowledgements

In the course of my research, the length of time used was proportionate to my appreciation in the importance of scientific investigation in the extension of life, which the author concluded was important.

My largest source of appreciation goes to my supervisor, Professor Peter Metcalfe from the University of Wollongong. My memories of him as a model Medical Physicist are most aptly described in this enduring word, “stoic”: *a philosopher holding virtue to the highest good and teaching indifference to pleasure and pain, one of great self control*. His advice was given in areas that included beam modelling, lateral thinking and scientific writing. That discussions were often made over coffee or tea, and occasionally over a biscuit, made research accessible and satisfying.

At the inevitable risk of unintentionally excluding people who have helped me or underestimating the value in the importance of the help afforded to me, I will attempt to write, in no order of importance, my acknowledgements in a concise manner to:

- Anatoly Rozenfeld, for his extensive knowledge in physics he shared to me
- Rashmi Gupta (St. George Hospital), for providing me with guidance in Pinnacle
- Wen Chuan Dong (Royal Hobart Hospital), for providing me with scientific discussions
- Robin Hill (Royal Prince Alfred Hospital), for the loan of the diamond detector
- Jim Boehm (St. George Hospital), for approval and discussion of my research and studies
- Bradley Oborn (St. George Hospital), for help with MATLAB and for useful discussions
- Nick Hardcastle (University of Wollongong), for his help with Pinnacle and Monte Carlo

A survey was made in the Pinnacle users email list which was instrumental to the study and many thanks extend to those who replied to me. Many thanks to my colleagues at the St. George Hospital for their role in training me as a Medical Physicist, with special mention to my former supervisors Ms. Feng Qin Chen and Ms. Gwi Ae Cho.

To those from whom I have received support from during my thesis, thank you. My family, extended family and close friends acted for my well-being. In particular, to those I have neglected when doing my research I would like to express my gratitude with the following: *I do not regret the things I've done, but those I did not do* (R. Cochrane).